Lewis-Acid Induced Disaggregation of Dimeric Arylantimony Oxides

Ralf Kather, Tomáš Svoboda, Maren Wehrhahn, Elena Rychagova,

Enno Lork, Libor Dostál, Sergey Ketkov and Jens Beckmann

Supplementary Material

Content

- Experimental section including the synthesis and characterization.

- Computational details including the results of MO, AIM, EDA calculations.

Experimental Section

General Procedures. All experiments were carried out under argon atmosphere using standard Schlenk techniques. Tris(pentafluorophenyl)borane,[S1] triphenylarsine oxide,[S2] triphenylstibine oxide[1] and 1,1'-(2-(oxostibanyl)-1,3-phenylene)bis(N,N-dimethylmethanamine)[15] were prepared according to literature. Dry solvents were collected from a SPS800 mBraun solvent system. ^{1}H-, ^{11}B-, ^{13}C- and ^{19}F-NMR spectra were recorded in CDCl$_3$ at r.t. using a Bruker Avance-360 spectrometer and are referenced to tetramethylsilane (^{1}H, ^{13}C), boron trifluoride diethyl etherate (^{11}B) and trichlorofluoromethane (^{19}F). Chemical shifts are reported in parts per million (ppm) and coupling constants (J) are given in Herz (Hz). For ESI-MS dichlormethane / acetonitrile solutions ($c = 1 \cdot 10^{-6}$ mol L^{-1}) were injected directly into the spectrometer at a flow rate of 3 μL min^{-1}. Nitrogen was used both as a drying gas and for nebulization with flow rates of approximately 5 L min^{-1} and a pressure of 5 spi, respectively. Pressure in the mass analyzer region was usually about $1 \cdot 10^{-5}$ mbar. IR spectra were recorded on a Perkin Elmer Spectrum 1000 FT-IR spectrometer as KBr discs and are reported in cm^{-1}. The melting point was determined using a Gallenkamp Melting Point Apparatus. Elemental analyses (C, H, N) were carried out by IWR, TU Wien, Austria using a Elementar Vario Macro instrument. The carbon percentage of **1** is lower than expected, which has been attributed to incomplete combustion. This observation has been made previously for compounds containing [B(C$_6$F$_4$)$_4$]$^-$ ions.[S3]

Synthesis of Ph$_3$AsOB(C$_6$F$_5$)$_3$. Tris(pentafluorophenyl)borane (300 mg, 0.586 mmol) and triphenylarsine oxide (189 mg, 0.581 mmol) stirred in 15 ml toluene at r.t. for 5 days. The solvent was removed under reduced pressure. The crude product was recrystallized from dichloromethane and *n*-hexane, affording Ph$_3$AsOB(C$_6$F$_5$)$_3$ as colorless crystals (333 mg, 0.399 mmol, 69 %, Mp. 191-193°C).

¹H-NMR: δ = 7.72-7.49 (m, 15H). **¹³C{¹H}-NMR:** δ = 148.1 (d, $^1J(^{19}F\text{-}^{13}C)$ = 243 Hz, CF), 139.6 (d, $^1J(^{19}F\text{-}^{13}C)$ = 248 Hz, CF), 137.3 (d, $^1J(^{19}F\text{-}^{13}C)$ = 237 Hz, CF), 134.2 (s, *p*-CH), 132.1 (s, *o*-CH or *m*-CH), 130.3 (s, *o*-CH or *m*-CH), 126.9 (s, *i*-C). **¹¹B{¹H}-NMR:** δ = -1.2 (s). **¹⁹F{¹H}-NMR:** δ = -133.6 (m, 2F, *o*-C_6F_5), -160.6 (tr, $^3J(^{19}F\text{-}^{19}F)$ = 20 Hz, 1F, *p*-C_6F_5), -166.0 (m, 2F, *m*-C_6F_5). **IR (KBr):** 3061 (w), 1645 (m), 1516 (m), 1465 (s), 1372 (w), 1314 (w), 1279 (m), 1096 (s), 972 (s), 930 (s), 791 (w), 769 (w), 738 (m), 673 (m), 614 (w), 574 (w), 467 (m). **ESI MS** (CH₂Cl₂/MeCN 1:10, negative mode): *m/z* = 868.8 ($C_{36}H_{15}AsBF_{15}OCl$) for [M+Cl]⁻. Anal. Calcd for $C_{36}H_{15}AsBF_{15}O$: C, 51.83; H, 1.81. Found: C, 51.11; H, 1.89.

Synthesis of Ph₃SbOB(C₆F₅)₃ (1). Tris(pentafluorophenyl)borane (300 mg, 0.586 mmol) and triphenylstibine oxide (216 mg, 0.293 mmol) stirred in 15 ml toluene at r.t. for 5 days. The solvent was removed under reduced pressure. The crude product was recrystallized twice from dichloromethane and *n*-hexane, affording Ph₃SbOB(C₆F₅)₃ (**1**) as colourless crystals (339 mg, 0.385 mmol, 66 %, Mp. 175-177°C).

¹H-NMR: δ = 7.79-7.47 (m, 15H). **¹³C{¹H}-NMR:** δ = 147.9 (d, $^1J(^{19}F\text{-}^{13}C)$ = 246 Hz, CF), 139.3 (d, $^1J(^{19}F\text{-}^{13}C)$ = 248 Hz, CF), 137.2 (d, $^1J(^{19}F\text{-}^{13}C)$ = 236 Hz, CF), 134.5 (s, *o*-CH or *m*-CH), 134.2 (s, *p*-CH), 131.0 (s, *o*-CH or *m*-CH), 126.8 (s, *i*-C). **¹¹B{¹H}-NMR:** δ = -0.9 (s). **¹⁹F{¹H}-NMR:** δ = -134.3 (m, 2F, *o*-C_6F_5), -161.0 (tr, $^3J(^{19}F\text{-}^{19}F)$ = 20 Hz, 1F, *p*-C_6F_5), -165.8 (m, 2F, *m*-C_6F_5). **IR (KBr):** 3062 (w), 1643 (m), 1514 (s), 1465 (s), 1337 (w), 1275 (m), 1090 (s), 974 (s), 913 (s), 826 (w), 766 (w), 733 (s), 685 (s), 446 (m). **ESI MS** (CH₂Cl₂/MeCN 1:10, negative mode): *m/z* = 916.7 ($C_{36}H_{15}SbBF_{15}OCl$) for [M+Cl]⁻. Anal. Calcd for $C_{36}H_{15}BF_{15}OSb$: C, 49.08; H, 1.72. Found: C, 46.76; H, 1.98 (see comment above).

Synthesis of 2,6-(CH₂NMe₂)₂C₆H₃SbOB(C₆F₅)₃ (2). Tris(pentafluorophenyl)borane (174 mg, 0.340 mmol) and the dimeric organoantimony(III) oxide (111 mg, 0.170 mmol) stirred in 15 ml toluene at r.t. for 5 days. The solvent was removed under reduced pressure. The crude product was recrystallized twice from dichloromethane and *n*-hexane, affording 2,6-(CH₂NMe₂)₂C₆H₃SbOB(C₆F₅)₃ **(2)** as colourless crystals (170 mg, 0.202 mmol, 60 %, Mp.156-158°C).

¹H-NMR: δ = 7.33-7.06 (m, 3H, CH), 4.02-3.54 (m, 4H, CH₂), 2.58-2.19 (m, 12H, CH₃).
¹³C{¹H}-NMR: δ = 154.8 (s, *i*-C), 148.1 (d, $^1J(^{19}F-^{13}C)$ = 237 Hz, CF), 145.5 (s, CH), 136.6 (d, $^1J(^{19}F-^{13}C)$ = 247 Hz, CF), 129.9 (s, CH), 126.0 (s, CH), 64.0 (s, CH₂N), 44.1 (s, N(CH₃)₂). **¹¹B{¹H}-NMR:** δ = -1.4 (s). **¹⁹F{¹H}-NMR:** δ = -134.5 (m, 2F, *o*-C₆F₅), -163.0 (m, 1F, *p*-C₆F₅), -167.1 (m, 2F, *m*-C₆F₅). **IR (KBr):** 3675 (w), 2924 (m), 1642 (m), 1514 (s), 1462 (s), 1358 (m), 1218 (w), 1176 (w), 1083 (s), 1031 (m), 961 (s), 835 (m), 769 (m), 745 (w), 735 (w), 684 (m), 670 (m), 631 (w), 601 (w), 573 (w), 511 (w), 454 (m). **ESI MS** (CH₂Cl₂/MeCN 1:10, positive mode): *m/z* = 329.1 (C₁₂H₂₀N₂SbO) for [RSbO+H]⁺. Anal. Calcd for C₃₀H₁₉BF₁₅N₂OSb: C, 42.84; H, 2.28; N, 3.33. Found: C, 43.22; H, 2.31; N, 3.01.

Crystallography. Intensity data of Ph₃AsOB(C₆F₅)₃, **1** and **2** were collected on Siemens P4 diffractometer at 173 K with graphite-monochromated Mo-Kα (0.7107 Å) radiation. All structures were solved by direct methods and refined based on F^2 by use of the SHELX program package as implemented in WinGX.[S4] All non-hydrogen atoms were refined using anisotropic displacement parameters. Hydrogen atoms attached to carbon atoms were included in geometrically calculated positions using a riding model. Defuse electron density related to highly disordered solvent molecules was accounted using the SQUEZZE routine.[S5] Crystal and refinement data are collected in Table S1. Figures were created using

DIAMOND.[S6] Crystallographic data (excluding structure factors) for the structural analyses

have been deposited with the Cambridge Crystallographic Data Centre.

Copies of this information may be obtained free of charge from The Director, CCDC, 12

Union Road, Cambridge CB2 1EZ, UK (Fax: +44-1223-336033; e-mail:
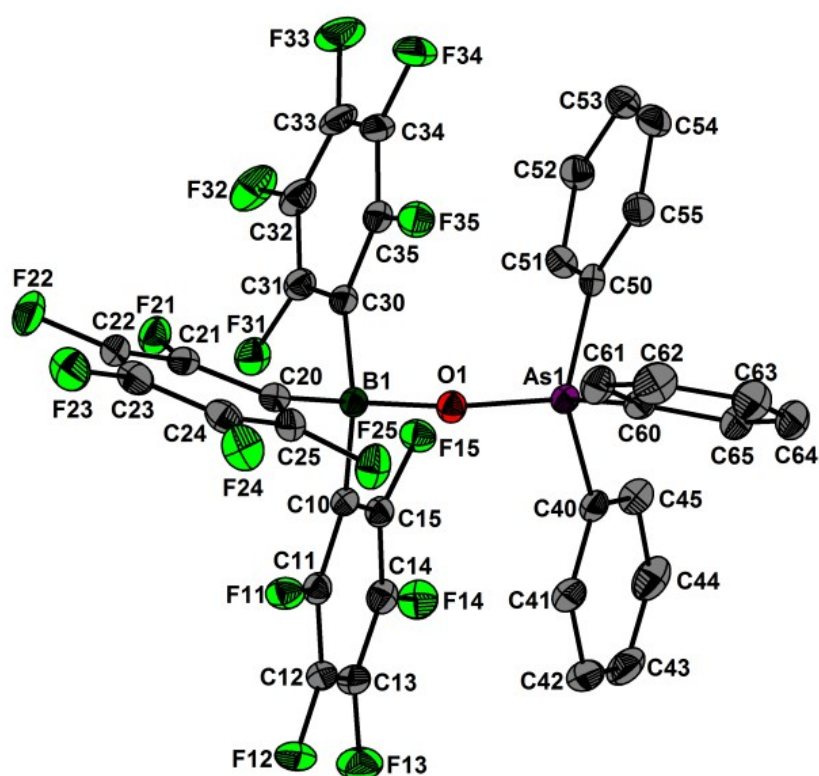
deposit@ccdc.cam.ac.uk or http://www.ccdc.cam.ac.uk).

Figure S1.   Molecular structure of $Ph_3AsOB(C_6F_5)_3$ showing 30% probability ellipsoids
and the crystallographic numbering scheme. Selected bond parameters [Å, °]: B1-O1
1.521(3), As1-O1 1.698(2), B1-O1-As1 134.0(2).

Table S1.   Crystal data and structure refinement of $Ph_3AsOB(C_6F_5)_3$, **1** and **2**.

	$Ph_3AsOB(C_6F_5)_3$	1	2
Formula	$C_{36}H_{15}AsBF_{15}O$	$C_{36}H_{15}BF_{15}OSb$	$C_{30}H_{19}BF_{15}N_2OSb$
Formula weight, g mol^{-1}	834.21	881.04	841.03
Crystal system	Monoclinic	Monoclinic	Triclinic
Crystal size, mm	$1.0 \times 0.6 \times 0.3$	$1.0 \times 0.8 \times 0.6$	$1.0 \times 0.8 \times 0.6$
Space group	$P2_1/n$	$P2_1/n$	P-1
a, Å	13.134(2)	12.248(2)	9.814(2)
b, Å	16.309(5)	17.312(4)	10.784(2)
c, Å	14.601(2)	15.058(4)	16.680(2)
α, º	90	90	84.080(10)
β, º	96.17(1)	95.34(1)	87.260(10)
γ, º	90	90	77.49(2)
V, Å^3	3110(1)	3179(1)	1713.6(5)
Z	4	4	2
ρ_{calcd}, Mg m^{-3}	1.782	1.841	1.630
μ (Mo $K\alpha$), mm^{-1}	1.216	0.988	0.914
$F(000)$	1648	1720	824
θ range, deg	2.54 to 27.50	2.05 to 27.52	2.05 to 27.52
Index ranges	$-16 \leq h \leq 16$	$-15 \leq h \leq 15$	$-12 \leq h \leq 12$
	$0 \leq k \leq 21$	$0 \leq k \leq 22$	$-13 \leq k \leq 13$
	$0 \leq l \leq 18$	$0 \leq l \leq 19$	$0 \leq l \leq 21$
No. of reflns collected	7128	7293	7845
Completeness to θ_{max}	99.8%	99.8%	99.8%
No. indep. Reflns	7128	7293	7845
No. obsd reflns with ($I>2\sigma(I)$)	5090	6004	7237
No. refined params	487	487	455
GooF (F^2)	1.012	1.037	1.064
R_1 (F) ($I > 2\sigma(I)$)	0.0428	0.0363	0.0302
wR_2 (F^2) (all data)	0.1035	0.0956	0.0829
Largest diff peak/hole, e Å^{-3}	0.331 / -0.512	0.588 / -0.541	0.460 / -0.760
CCDC number	1045570	1045571	1045572

Computational details. The geometries of the compounds studied were optimized at the M062X/DGDZVP level of theory employing the Gaussian09 code[S7] with the ultrafine integration grid and using the X-ray structures as the starting point. The frequency calculations were performed to check whether the structure found corresponds to the energy minimum. The wavefunctions obtained were then used for the electron density topology analysis and the potential energy density / kinetic energy density ratio computations with the AIMALL package.[S8] The deformation densities were obtained with the Multiwfn program[S9] by subtracting the ρ values of the individual sphericalized atoms from the total molecular electron density. We used the atomic ρ values calculated at the M062X/DGDZVP level of theory. To estimate the B-O bond energies in the $Ph_3EOB(C_6F_5)_3$ (E= P, As, Sb) complexes, the energies of the optimized Ph_3EO and $B(C_6F_5)_3$ were subtracted from the $Ph_3EOB(C_6F_5)_3$ energy. The counterpoise correction[S10] was calculated separately to take the basis set superposition error (BSSE) into consideration. For the energy decomposition analysis (EDA), the complexes were re-optimized with the ADF2013.01 code[S11] at the PW91/DZP level of DFT. Then the EDA procedure was performed for the Ph_3EO (E = P, As, Sb) or 2,6-$(Me_2NCH_2)_2C_6H_3SbO$ and the $B(C_6F_5)_3$ fragments at the same level of theory using the Morokuma method.[S12] The resulting total interaction energy is equal to the bond snapping energy which corresponds to the reaction of formation of a complex from the individual fragments possessing the same structural parameters as those in the complex.[S12]

Table S2. Selected calculated and experimental bond lengths (Å) and bond angles (degrees).

Molecule	M062X/DGDZVP				Experiment			
	E-O	E-C[a]	B-O	E-O-B	E-O	E-C[a]	B-O	E-O-B
Ph_3PO / $Ph_3POB(C_6F_5)_3$	1.496 /1.535	1.816 / 1.798	- / 1.556	- / 149.5	1.487/ 1.497	1.800 / 1.787	- / 1.538	- / 178.7
Ph_3AsO / $Ph_3AsOB(C_6F_5)_3$	1.645/ 1.710	1.929/ 1.910	- / 1.518	- / 130.9	1.645 / 1.701	1.898 / 1.910	- / 1.536	- / 134.8
Ph_3SbO / $Ph_3SbOB(C_6F_5)_3$	1.845 / 1.899	2.126 / 2.104	- / 1.504	- / 131.6	- / 1.877	- / 2.095	- / 1.508	- / 132.0
$(Ph_3SbO)_2$	2.029 [a]	2.145	-	-	2.005 [a]	2.141	-	-
ArSbO / $ArSbOB(C_6F_5)_3$	1.866/ 1.931	2.172/ 2.125	- / 1.475	- / 135.0	- / 1.921	- / 2.099	- / 1.473	- / 134.0
$(ArSbO)_2$	2.038 [a]	2.180	-	-	2.009 [a]	2.171	-	-

[a]- averaged interatomic distances. Ar = 2,6-$(Me_2NCH_2)_2C_6H_3$

Table S3. The electron density ρ (a.u.) and the potential energy density / kinetic energy density ratio |V|/G in the E-O and E-C bonding critical points.

Molecule	ρ			|V|/G	
	E-O	E-C[a]	B-O	E-O	E-C[a]
Ph_3PO / $Ph_3EOB(C_6F_5)_3$	0.223 / 0.196	0.166 / 0.175	- / 0.108	1.374 / 1.369	2.292 / 2.366
Ph_3AsO / $Ph_3AsOB(C_6F_5)_3$	0.211/ 0.176	0.144/ 0.150	- / 0.129	1.562 / 1.494	1.920/ 2.037
Ph_3SbO / $Ph_3SbOB(C_6F_5)_3$	0.156 / 0.134	0.111/ 0.117	- / 0.135	1.314 /1.260	1.673/ 1.741
$(Ph_3SbO)_2$	0.117; 0.085	0.106		1.309; 1.292	1.780
ArSbO / $ArSbOB(C_6F_5)_3$	0.147/ 0.122	0.101/ 0.111	- / 0.147	1.285 / 1.234	1.595/ 1.645
$(ArSbO)_2$	0.100	0.086		1.251	1.627

[a]- averaged values. Ar = 2,6-$(Me_2NCH_2)_2C_6H_3$

Table S4. Mulliken (M062X/DGDZVP) and AIM charges of selected atoms.

Molecule	Mulliken			AIM		
	E	O	B	E	O	B
Ph_3PO / $Ph_3EOB(C_6F_5)_3$	+1.05/ +1.15	-0.69 / -0.70	- / +0.57	+3.09 / +2.68	-1.51 / -1.54	- / +2.07
Ph_3AsO / $Ph_3AsOB(C_6F_5)_3$	+0.80 / +0.81	-0.70 / -0.64	- / +0.58	+2.12 / +2.06	-1.20 / -1.33	- / +2.01
Ph_3SbO / $Ph_3SbOB(C_6F_5)_3$	+1.04 / +1.23	-0.79 / -0.78	- / +0.56	+2.36 / +2.39	-1.23 / -1.38	- / +2.02
$(Ph_3SbO)_2$	+1.27	-1.00[a]	-	+2.58	-1.38[a]	-
ArSbO / $ArSbOB(C_6F_5)_3$	+0.75/ +0.82	-0.88 / -0.78	- /+0.62	+1.64 / +1.77	-1.29 / -1.43	- / +2.03
$(ArSbO)_2$	+0.97	-1.02[a]	-	+1.82	-1.38[a]	-

[a]- averaged values. Ar = 2,6-$(Me_2NCH_2)_2C_6H_3$

Table S5. Energy decomposition analysis according to the Morokuma scheme[10] at the PW91/DZP level of theory (kcal mol^{-1}).

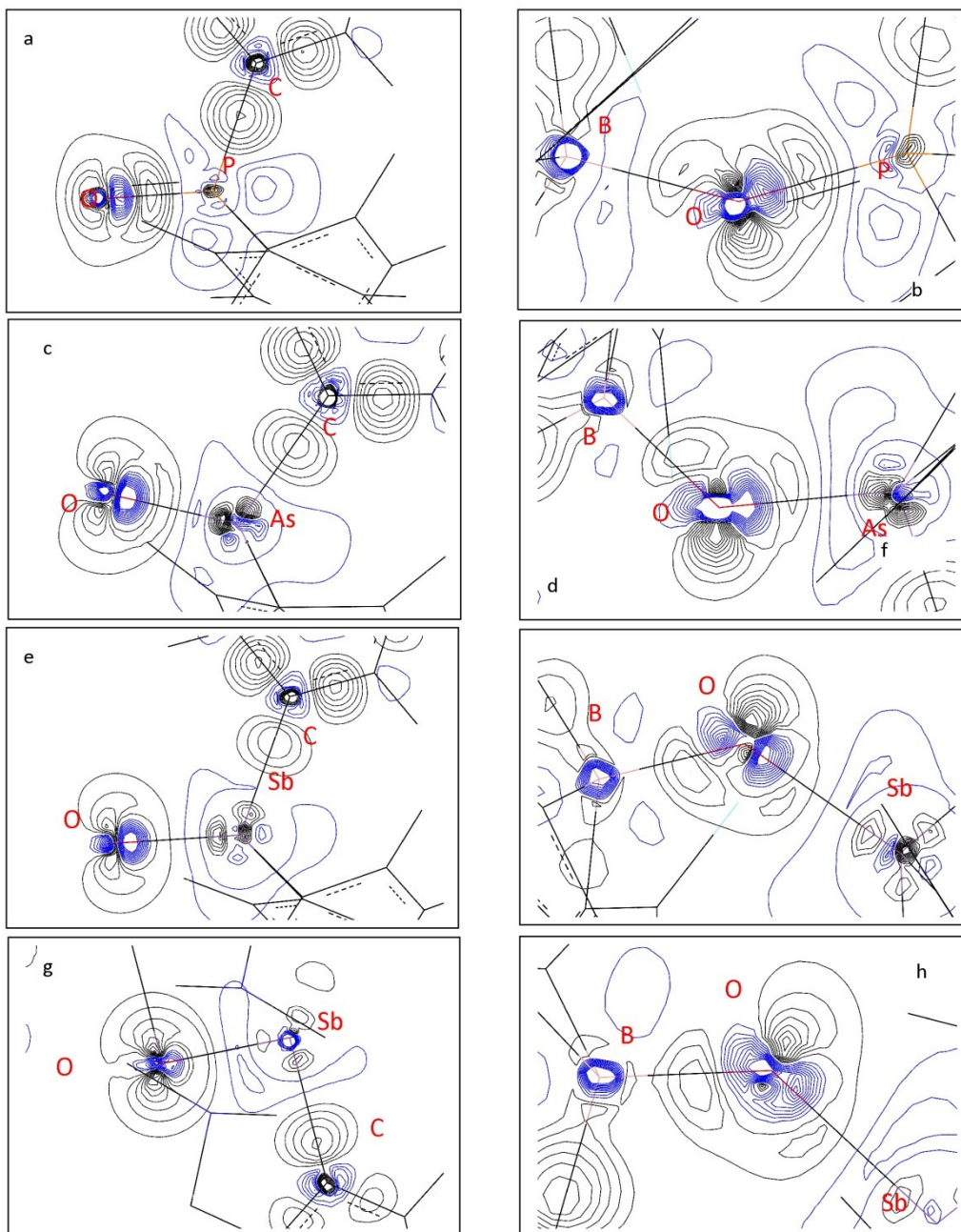|	$Ph_3POB(C_6F_5)_3$	$Ph_3AsOB(C_6F_5)_3$	$Ph_3SbOB(C_6F_5)_3$	$ArSbOB(C_6F_5)_3$
Pauli repulsion ΔE_{Pauli}	166.9	184.6	185.7	219.4
Electrostatic interactions ΔE_{elstat}	-103.2	-121.7	-124.5	-147.0
Steric interactions ΔE_{steric}	63.7	62.9	61.2	72.4
Orbital interactions ΔE_{orb}	-111.5	-133.3	-140.6	-163.6
Total interaction energy ΔE_{int}	-47.8	-70.4	-79.5	-91.2

Figure S2. Profiles of the deformation electron density (0.01-0.1 a.u., step 0.01 a.u.; black-positive, blue-negative) for (a) Ph$_3$PO (b) Ph$_3$POB(C$_6$F$_5$)$_3$ (c) Ph$_3$AsO (d) Ph$_3$AsOB(C$_6$F$_5$)$_3$, (e) Ph$_3$SbO, (f) Ph$_3$SbOB(C$_6$F$_5$)$_3$ (**1**), (g) (Ph$_3$SbO)$_2$ and (h) 2,6-(Me$_2$NCH$_2$)$_2$C$_6$H$_3$SbOB(C$_6$F$_5$)$_3$ (**2**) in the OEC plane (E=P, As, Sb) for the oxides and EOB plane for the boron complexes.
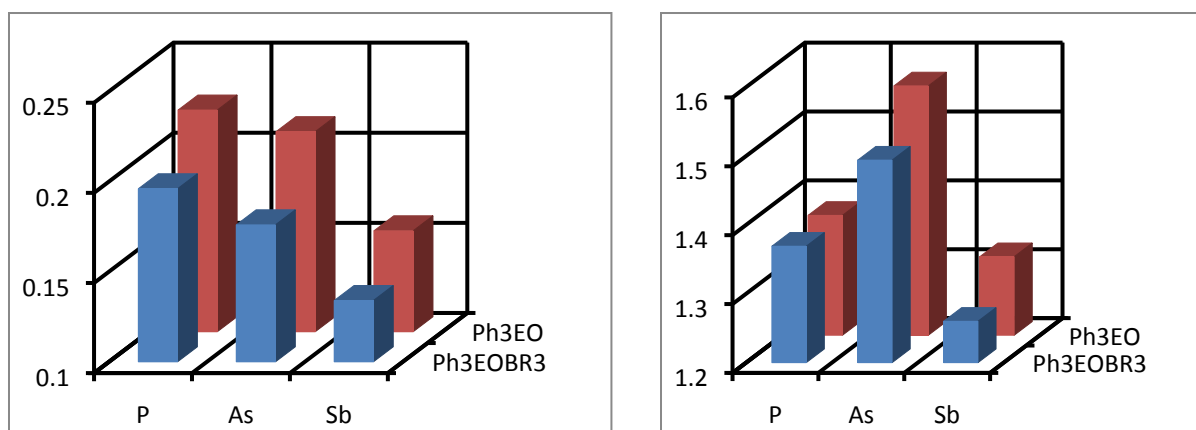
Figure S3. The electron density (a.u.) (left) and the $|V(\mathbf{r}_c)| / G(\mathbf{r}_c)$ ratio at the E-O bonding critical points of Ph_3EO and $Ph_3EOB(C_6F_5)_3$.
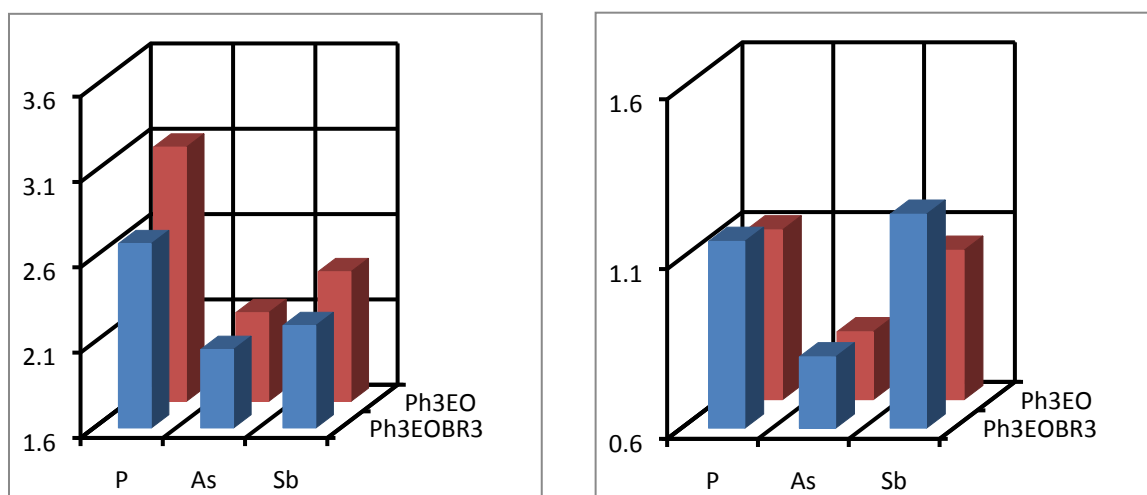

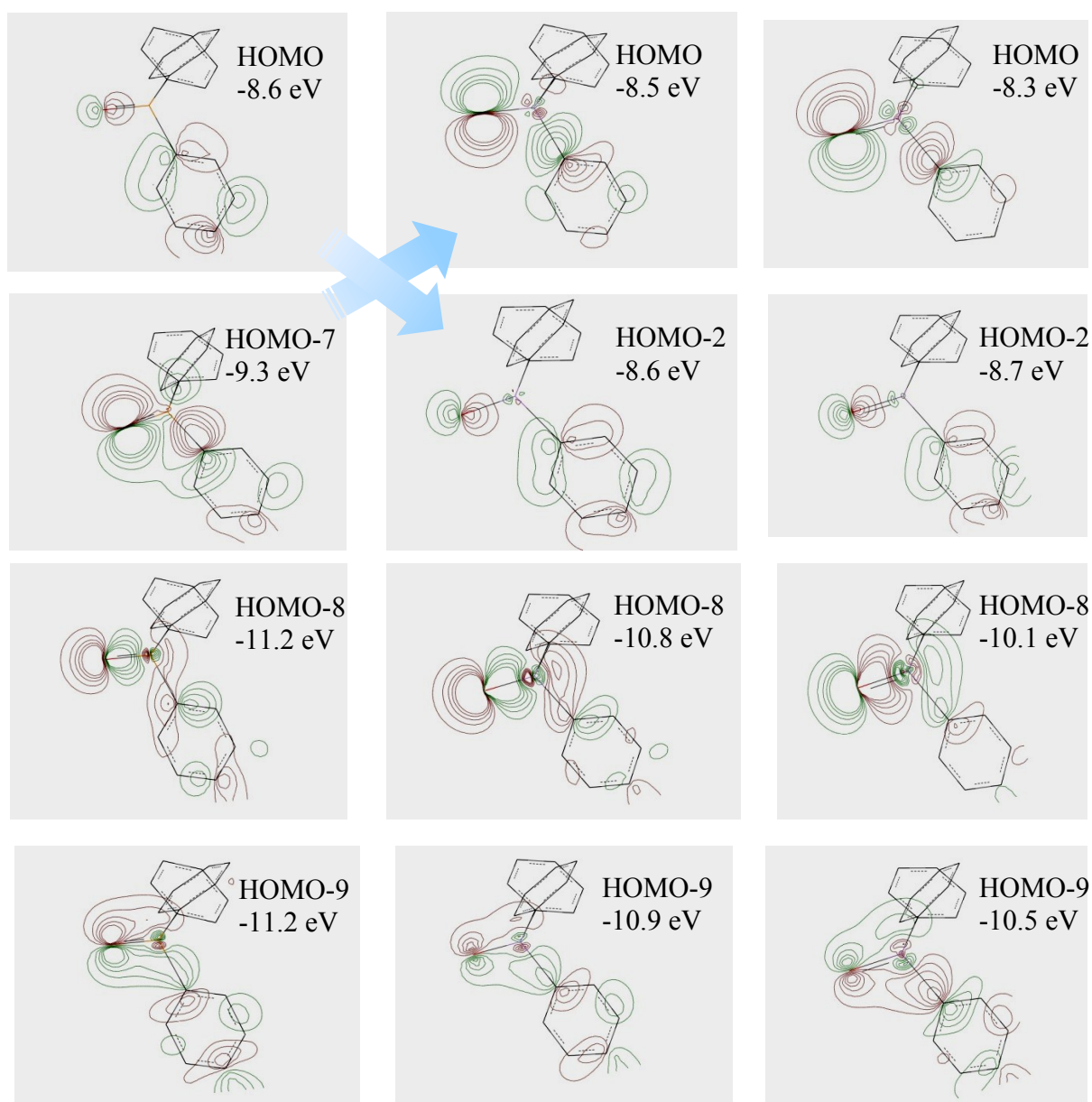**Figure S4.** Mulliken (left) and AIM (right) charges of P, As and Sb in monomeric Ph_3EO and $Ph_3EOB(C_6F_5)_3$.

HOMO
-8.6 eV

HOMO
-8.5 eV

HOMO
-8.3 eV

HOMO-7
-9.3 eV

HOMO-2
-8.6 eV

HOMO-2
-8.7 eV

HOMO-8
-11.2 eV

HOMO-8
-10.8 eV

HOMO-8
-10.1 eV

HOMO-9
-11.2 eV

HOMO-9
-10.9 eV

HOMO-9
-10.5 eV

Ph3PO☐   Ph3AsO☐   Ph3SbO

Figure S5.   Contour maps in the EOC planes (0.02-0.1 a.u., step 0.02 a.u., red positive, green negative) and energies of selected MOs for monomeric Ph$_3$EO (E = P, As, Sb).

References

[S1]   (a) A. G. Massey, A. J. Park, *J. Org. Chem*. **1964**, *2*, 245. (b) M. Kuprat, M. Lehmann, A. Schulz, A. Villinger, *Organometallics* **2010**, *29*, 1421.

[S2]   R. L. Shriner, C. N. Wolf, *Org. Syn.* **1950**, *30*.

[S3]   A. Marco, R. Compañó, R. Rubio, I. Casals *Microchim. Acta* **2003**, *142*, 13.

[S4]   (a) G. M. Sheldrick *Acta Cryst*. **2008**, *A64*, 112. (b) L. J. Farrugia *J. Appl. Crystalogr*. **1999**, *32*, 837.

[S5]   (a) A. Spek *J. Appl. Cryst*. **2003**, *36*, 7. (b) P. van der Sluis, A. L. Spek *Acta Cryst*. **1990**, *A46*, 194.

[S6]   K. Brandenburg, H. Putz, DIAMOND V3.1d, Crystal Impact GbR, **2006**.

[S7]   Gaussian 09, Revision B.01, M. J. Frisch, G. W. Trucks, H. B. Schlegel, G. E. Scuseria, M. A. Robb, J. R. Cheeseman, G. Scalmani, V. Barone, B. Mennucci, G. A. Petersson, H. Nakatsuji, M. Caricato, X. Li, H. P. Hratchian, A. F. Izmaylov, J. Bloino, G. Zheng, J. L. Sonnenberg, M. Hada, M. Ehara, K. Toyota, R. Fukuda, J. Hasegawa, M. Ishida, T. Nakajima, Y. Honda, O. Kitao, H. Nakai, T. Vreven, J. A. Montgomery, Jr., J. E. Peralta, F. Ogliaro, M. Bearpark, J. J. Heyd, E. Brothers, K. N. Kudin, V. N. Staroverov, R. Kobayashi, J. Normand, K. Raghavachari, A. Rendell, J. C. Burant, S. S. Iyengar, J. Tomasi, M. Cossi, N. Rega, J. M. Millam, M. Klene, J. E. Knox, J. B. Cross, V. Bakken, C. Adamo, J. Jaramillo, R. Gomperts, R. E. Stratmann, O. Yazyev, A. J. Austin, R. Cammi, C. Pomelli, J. W. Ochterski, R. L. Martin, K. Morokuma, V. G. Zakrzewski, G. A. Voth, P. Salvador, J. J. Dannenberg, S. Dapprich, A. D. Daniels, Ö. Farkas, J. B. Foresman, J. V. Ortiz, J. Cioslowski, and D. J. Fox, Gaussian, Inc., Wallingford CT, **2010**.

[S8]   AIMAll (Version 13.05.06), T.A. Keith, TK Gristmill Software, Overland Park KS, USA, **2013**, http://aim.tkgristmill.com.

[S9]   (a) T. Lu, F. Chen *J. Comp. Chem*. **2012**, *33*, 580. (b) *Lu, F. Chen J. Mol. Graph. Model*. **2012**, *38*, 314.

[S10]   F.B. Van Duijneveldt, J.G.C.M. van Duijneveldt-van de Rijdt, J.H. van Lenthe, *Chem. Rev*. **1994**, *94*, 1873.

[S11]   (a) E.J. Baerends, T. Ziegler, J. Autschbach, D. Bashford, A. Bérces, F.M. Bickelhaupt, C. Bo, P.M. Boerrigter, L. Cavallo, D.P. Chong, L. Deng, R.M. Dickson, D.E. Ellis, M. van Faassen, L. Fan, T.H. Fischer, C. Fonseca Guerra, M. Franchini, A. Ghysels, A. Giammona, S.J.A. van Gisbergen, A.W. Götz, J.A. Groeneveld, O.V. Gritsenko, M. Grüning, S. Gusarov, F.E. Harris, P. van den Hoek, C.R. Jacob, H. Jacobsen, L. Jensen, J.W. Kaminski, G. van Kessel, F. Kootstra, A. Kovalenko, M.V. Krykunov, E. van Lenthe, D.A. McCormack, A. Michalak, M. Mitoraj, S.M. Morton, J. Neugebauer, V.P. Nicu, L. Noodleman, V.P. Osinga, S. Patchkovskii, M. Pavanello, P.H.T. Philipsen, D. Post, C.C. Pye, W. Ravenek, J.I. Rodríguez, P. Ros, P.R.T. Schipper, H. van Schoot, G. Schreckenbach, J.S. Seldenthuis, M. Seth, J.G. Snijders, M. Solà, M. Swart, D. Swerhone, G. te Velde, P. Vernooijs, L. Versluis, L. Visscher, O. Visser, F. Wang, T.A. Wesolowski, E.M. van Wezenbeek, G. Wiesenekker, S.K. Wolff, T.K. Woo, A.L. Yakovlev, ADF2013.01, SCM, Theoretical Chemistry, Vrije Universiteit, Amsterdam, The Netherlands, http://www.scm.com. (b) G. te Velde, F.M. Bickelhaupt, S.J.A. van Gisbergen, C. Fonseca Guerra, E.J. Baerends, J.G. Snijders and T. Ziegler, Chemistry with ADF, Journal of Computational Chemistry **2001**, *22*, 931.

[S12]   (a) K. Morokuma, *J. Chem. Phys*. **1971**, *55*, 1236. (b) K. Morokuma and K. Kitaura, in Chemical Applications of Atomic and Molecular Electronic Potentials, edited by P. Politzer and D. G. Truhlar Plenum, New York, **1981**, p. 215. (c) T. Ziegler, A. Rauk *Theor. Chim. Acta*, **1977**, *46*, 1. (d) T. Ziegler and A. Rauk *Inorg. Chem*. **1979**, *18*,

1755. (e) F.M. Bickelhaupt, E.J. Baerends, In: *Rev. Comput. Chem.*; K.B. Lipkowitz, D.B. Boyd, Eds.; Wiley, New York, **2000**, Vol. 15, p.1-86.